IIETA International Information and Engineering Technology Association
Advancing the World of Information and Engineering

Instrumentation Mesure Métrologie
Vol. 24, No. 6, December, 2025, pp. 361-370
Journal homepage: http://iieta.org/journals/i2m

Predictive Corrosion Degradation Modelling of Oil Country Tubular Goods Using Physics-Informed Machine Learning and Digital Twin Technologies

Mohammed Jasim Aljumaili[1], Hiba A. Abdalwahhab[2], Hyman Jafar Meerza[2], Mohammed Ali Abdulrehman[2,3*], Ahmed Subhi Abbas[4], Dar Ali Yousif[5]

[1] Biomedical Engineering Research Center, University of Anbar, Ramadi 31001, Iraq
[2] Department of Materials Engineering, College of Engineering, Mustansiriyah University, Baghdad 10045, Iraq
[3] School of Materials and Mineral Resources Engineering, Universiti Sains Malaysia (USM), Penang 14300, Malaysia
[4] Department of Civil Engineering, College of Engineering, Al-Mustafa University, Baghdad 10045, Iraq
[5] Department of Air Conditioning and Refrigeration Technologies, College of Engineering, Alsalam University College, Baghdad 10010, Iraq

Corresponding Author Email: mohammed_ali_mat@uomustansiriyah.edu.iq

https://doi.org/10.18280/i2m.240603

Received: 1 September 2025
Revised: 12 October 2025
Accepted: 20 October 2025
Available online: 31 December 2025

Keywords:
physics-informed machine learning, digital twin, fatigue–corrosion interaction, Inconel 625, duplex stainless steel

ABSTRACT

This study provides a comprehensive research methodology to accurately determine the degradation and remaining life of Oil Country Tubular Goods (OCTG) under sour and high-temperature conditions. Experiments were conducted to determine the properties of three materials (API X70 Carbon Steel, 22Cr duplex stainless steel, and Inconel 625). The results confirmed that Inconel 625 possessed the maximum hardness and resistance to corrosion, followed by 22Cr duplex stainless steel and API X70 Carbon Steel. A physics-informed long short-term memory (PI-LSTM) algorithm was developed for physically grounded estimation by incorporating Paris's law and Arrhenius models for corrosion. The algorithm outperformed all conventional models (accuracy-93% and R^2-0.92), enabled reliable life estimation in digital twin simulation platforms, and allowed precise estimation of degradation performance ±10% accuracy, replicating laboratory experiments. The digital twin simulation estimated the pipeline health index values to provide reliable predictive maintenance services. The methodology provides efficient research for scaling intelligent integrity management systems for OCTG under adverse operational conditions.

1. INTRODUCTION

The oil and gas industry must deal with more complicated and demanding conditions because it is looking for deeper reservoirs, and the world requires more energy to sustain its growth. Sour service environments are some of the most difficult to work in because high temperatures, high pressures, and corrosive substances such as hydrogen sulfide (H_2S), carbon dioxide (CO_2), and chlorides work together to accelerate the breakdown of Oil Country Tubular Goods (OCTG). These are important steel components that maintain wellbore stability during drilling and production. This is because there are numerous ways in which things can break down, and they play off each other. These include uniform corrosion, localized pitting, stress corrosion cracking (SCC), sulfide stress cracking (SSC), hydrogen-induced cracking (HIC), and corrosion-fatigue coupling. Such processes compromise the structural integrity of wells and pipelines and predispose them to disastrous failures that can have both environmental and financial consequences [1, 2].

The primary approaches to traditional maintenance and qualification work consist of standardized laboratory tests and empirical correlations based on the number of years of industrial experience. These techniques have provided valuable data on the behavior of materials; however, because they are grounded in actual data, they are not always able to predict how materials will behave under varying conditions of service. Traditional testing or models at rest cannot wholly show alterations in the sour environment in terms of temperature, fluid chemistry, and stress. Consequently, maintenance approaches based on these techniques tend to either be overly conservative and costly, or fail to eliminate the possibility of failure too early [3, 4]. To overcome these issues, predictive models that integrate experimental data, physical theory, and real-time data of operations are needed to ensure a better demonstration of the degradation evolution.

Recently, through the integration of research in material science and artificial intelligence, a novel computational tool called physics-informed machine learning has emerged with impressive applications in the analysis of complex engineering systems. In contrast to purely data-driven approaches, PIML models involve the direct embedding of constitutive equations, conservation laws, or governing principles into the learning framework to ensure physically consistent solutions with high interpretability, even with limited data. PIML differs from traditional data-driven models in that it explicitly uses governing equations and constitutive relationships during the learning process. This means that the model can be

comprehended and obeys the simple laws of physics (even in cases where little data are available) owing to this integration [5, 6]. Such models can be used to describe fatigue crack propagation and corrosion kinetics using physically based constraints, such as the law of Paris and Arrhenius-type relations, in the context of OCTG reliability. PIML improves the prediction accuracy and helps reduce the incidence of nonphysical results by combining these equations into a learning system. The combination of real-world data obtained in the real world and mechanistic knowledge enables the development of both experimental validation and predictive analytics, which is its hybrid quality.

Digital twin technology also plays a significant role in data-driven reliability management. A digital twin refers to a model of a physical object that is computer-generated and evolves over time as it is continuously updated with field measurements obtained through sensors. In OCTG systems, digital twins integrate data on pressure, temperature, and chemical composition with predictive algorithms to determine the state of the material, its degradation, and its life expectancy. Constant monitoring and simulation enable engineers to enhance inspection and maintenance schedules [7, 8] to provide constant monitoring and risk estimation rather than adherence to defined timeframes. The addition of PIML to digital twin architectures produces models that can be modified and self-healed with shifts in operations. This enables the maintenance strategies to become more dependable and economical.

The combination of data analytics, computer modelling, and materials science is transforming energy sector operations. It has been shown that hybrid models that combine physical laws and machine learning algorithms offer greater adaptability, scalability, and interpretability. Such models dynamically adapt to service conditions, forming closed feedback loops that lead to improved safety and durability [9, 10]. Moreover, complex simulation procedures, such as Deep Fluids and hybrid damage identification algorithms, have demonstrated how deep neural networks can accurately recreate both thermomechanical and electrochemical processes with a high level of computational efficiency [11, 12]. Methods are necessary to record the mechanical and chemical interdependent degradation phenomena that govern the behavior of OCTGs.

Despite these improvements, research gaps remain significant. The majority of studies emphasize either PIML or digital twin technologies independently, which makes the approaches to this fragmented and thus fails to merge the experimental data on mechanical, electrochemical, and microstructural processes into a unified framework. In addition, many of these studies are limited to laboratory experiments or theoretical studies, which limits their extrapolation to field-scale operations, where loads and chemical compositions are variable [13, 14]. To overcome these limitations, the development of holistic hybrid systems that integrate continuous field data with physical degradation models is critical to making them adaptable and interpretable.

These gaps were directly filled in this study with a unified physics-constrained artificial intelligence and digital twin framework for predictive degradation assessment and lifespan optimization in OCTG systems operating under extreme service conditions. It is a framework that unites experimental characterization, machine learning, and physical modelling into one system capable of illustrating the breakdown of things in the real world. Constitutive relationships are involved in the learning process, which defines the distribution of fatigue cracks and the corrosion process. This ensures that model predictions are always physically consistent and reliable, irrespective of the conditions [15, 16]. The digital twin element implements a predictive structure by incorporating real-time field measurements to continuously refresh the degradation and remaining life projections to enable proactive maintenance and inspection scheduling based on risks.

The proposed study contributes to the enhancement of predictive reliability engineering by unifying physical principles, artificial intelligence, and real-time data analytics in a unified system. PIML and digital twin technologies represent a significant shift in asset management towards a proactive approach rather than a reactive one. This approach decreases unexpected downtimes, minimizes maintenance expenses, and enhances safety and environmental standards [17]. Along with OCTG systems, the general concept of this hybrid structure can be applied to other applications, including aerospace, transport, and biomedical engineering, in which materials must perform in harsh environments. This research paper is part of a worldwide movement in intelligent, sustainable, and resilient engineering systems that rely on physics-informed digital transformation, which combines real-world data with computer-based forecasts.

2. MATERIALS AND METHODS

2.1 Theoretical framework

To develop a prognostic framework for understanding degradation processes in OCTG under sour and high-temperature conditions from a fundamental viewpoint involving the interplay of fatigue loads and corrosion processes, it was necessary to embed two fundamental models related to degradation processes into the framework. The inclusion of these models to embed fundamental laws related to degradation processes provides prognostic reliability to ensure adherence to fundamental laws, even in complex situations involving high temperatures and sour service conditions. The two models selected to embed fundamental laws related to degradation processes in OCTG in sour and high-temperature service conditions were Paris's law for fatigue failure and Arrhenius models for degradation processes.

2.1.1 Fatigue crack growth kinetics

The rate of fatigue crack propagation in tubular steels subjected to cyclic loading conditions and corrosive media can be modelled according to Paris's law. This law links the rate of crack propagation to the stress intensity factor range (ΔK). The formula for this law can be written as:

$$da/dN = C\,(\Delta K)m \tag{1}$$

where, '*a*' denotes the instantaneous value of crack extension, '*N*' represents the number of loading cycles applied to cause material failure, "*ΔK*" stands for stress intensity factor intensity range values, and '*C* & *m*' denote material-related empirical values related to crack-resistant material property. The current research validates the continued application of Paris' law in appropriately analyzing the fatigue characteristics of high-strength steels and nickel alloys in sour service environments by considering the temperature and environmental variability associated with such materials [18,

19]. Negi et al. [18] successfully illustrated the utility of the phase-field model to investigate the rates of crack growth in OCTG steel samples under hydrogen sulfide environments and showed a very close resemblance between the stress intensity factor and hence confirmed the relevance of the Paris law. The study conducted by Jiang et al. [19] validated application of 'Paris law' in increased rate of crack development associated with 'pressure vessel material 4130X.' In cases of increased fatigue crack development, the material property simulation associated with the Paris law application's restricted physically invalid extrapolated values is used to ensure adherence to material property values correlated to the fatigue material property.

2.1.2 Temperature-dependent corrosion kinetics

Corrosion under sour environmental conditions is thermally activated, and its rate accelerates exponentially as the temperature increases. The predictive formula captures this dependence by involving the Arrhenius-type equation to represent the temperature effects on the reaction rate kinetics as follows:

$$CR(T) = A \exp(-E_a / (R\,T)) \quad (2)$$

where, $CR(T)$ represents the corrosion rate at temperature T, A is the pre-exponential factor describing the rate of molecular collisions responsible for corrosion, E_a corresponds to the activation energy of the rate-determining step of the process, R represents the ideal gas constant, and T represents the absolute temperature. Many studies have been conducted to effectively apply this formula to thermally accelerated corrosion processes of steels, nickel alloys, and titanium materials in oil fields and high-temperature applications [20]. Current research has also confirmed its relevance to digital twin and PIML models. To improve digital twin models related to gas turbine machinery components, Farhat and Altarawneh [21] applied degradation kinetics based on the Arrhenius formula. Including temperature dependence improves the accuracy of the models related to oxidation and corrosion fatigue. In this study, Parsa [22] confirmed the generalizability of PIML models following Arrhenius-type degradation kinetics to several thermal ranges for energy systems by describing the material degradation processes under high-temperature conditions. The values of A and E_a were experimentally estimated via electrochemical tests performed over certain temperature ranges to provide the necessary adjustments to the thermal acceleration of the digital twin models. The application of such dependence provides relevant digital twin results for material degradation processes under high-temperature conditions, instead of strictly defining it via data inference methods by capturing robustness in physically grounded models.

The combination of Paris' fatigue law and Arrhenius corrosion kinetics provides a theoretical basis for a hybrid physics-informed model. A dual-constraint methodology ensures that the learning algorithm not only predicts data truthfully but also complies with fundamental physical equations describing material behavior in mechanical and electrochemical degradation processes. The combination of these equations in the digital twin architecture allows the construction of physically sound and interpretable representations of degradation processes for different service conditions of OCTG materials over broad intervals of time and wide ranges of loading to provide new solutions matching state-of-the-art research in materials predictive science and physically informed AI systems [18, 21, 22].

2.2 Material selection and specimen preparation

The specimen materials were selected and prepared according to the research question and purpose. Material Selection and Preparation of the Specimen: 2.2 The selection and preparation of the specimen material were based on the research question and purpose of the research.

To determine the various mechanical properties and corrosion resistance characteristics pertinent to the application of OCTG in sour and high-temperature conditions, three representative alloy systems were chosen. These were microalloyed API X70 carbon steel, 22Cr duplex stainless steel (UNS S31803), and nickel-based superalloy Inconel 625 (UNS N06625). They were selected based on their progressive increase in mechanical strength, corrosion resistance, and CO_2/H_2S stability.

Recent studies have verified the appropriateness of such alloys for sour and high-pressure services. Negi et al. [18] showed that duplex and nickel-based alloys are effective in mitigating SSC in hydrogen sulfide conditions. Jiang et al. [19] showed that microstructural refinement and inclusion distribution have an important influence on the fatigue crack growth resistance of high-strength steels, including API X70. Farhat and Altarawneh [21] and Pars [22] also asserted that Inconel 625 exhibits better performance in coupled thermal-corrosive environments because of its high Ni-Cr-Mo content, which facilitates the formation of a stable passive layer that inhibits localized corrosion.

Tubular stock materials were milled to standardized geometries for various experimental programs. Quasistatic testing of uniaxial dog-bone tensile specimens was performed in compliance with ASTM E8 [23], and axial fatigue testing was performed in compliance with ASTM E466 [24] to obtain a consistent stress distribution during cyclic loading. Electrochemical characterization of rectangular corrosion coupons measuring 10 × 20 × 3 mm was performed using the surface area control recommendations of ASTM G1 [25]. Moreover, short-ring sections of the tubes were fabricated to test the hydrostatic pressure and collapse under conditions close to the loading conditions of downhole tubules in service.

Each sample was successively ground in silicon carbide abrasive papers up to 1200-grit, followed by polishing in a 1 µm alumina suspension to achieve a consistent mirror finish. Controlling the surface roughness is also necessary because surface asperities may act as preferential corrosion initiators and crack nucleation locations. Recent studies have shown that the surface finish is a critical aspect of the fatigue and corrosion performance of high-strength steels and nickel alloys [19].

Each specimen was polished and ultrasonically washed with acetone and ethanol to eliminate particulate and organic contaminants, respectively. The samples were then dried under a high-purity nitrogen stream to avoid oxidation and tested. These cleaning and preparation procedures were in accordance with ASTM G1 standards and the most recent best-practice guidelines on the use of corrosion-fatigue assessment of OCTG products [18, 20].

This careful preparation ensured that all samples had similar surface quality and dimensional precision, minimizing experimental variability and allowing for a comparison of the mechanical and electrochemical performance. The resulting

specimens provided a uniform foundation for the subsequent testing stages, which were integrated into the physics-informed digital twin model developed in this study.

2.3 Mechanical characterization

The mechanical characterization of the various elements is provided to enable the mechanical modelling of the gas and oil extraction processes.

Mechanical tests were conducted to determine the responses of the selected OCTG alloys to tensile, fatigue, and creep tests under controlled conditions. All the procedures were in line with the relevant ASTM standards to ensure that they were performed and redoubled.

Tensile tests at room temperature provided the yield strength, ultimate tensile strength, and elongation according to ASTM E8. API X70 possesses a balance between strength and ductility, duplex stainless steel possesses higher yield strength and moderate elongation, and Inconel 625 possesses better tensile performance and structural stability [18, 19].

The fatigue tests were based on ASTM E466 and were conducted under load-controlled cyclic testing. Duplex stainless steel has the highest resistance to fatigue, and Inconel 625 maintains a stable cyclic performance, indicating that it is highly resistant to corrosion [21].

According to ASTM E139 [26], the creep behavior was investigated at 600°C and at a constant load. Inconel 625 was highly resistant to high temperatures, and it was not easy to deform; however, carbon steel would deform because the grains moved on the boundary [20].

Overall, the mechanical findings indicate that Inconel 625 and duplex stainless steel are more effective for sour and high-temperature OCTG applications. This renders them profitable for forecasting long-term degradation that will occur in the long term.

2.4 Electrochemical characterization

To test the corrosion behavior of the selected OCTG alloys under simulated sour service conditions, electrochemical testing was conducted. A temporal variation in the parameters of the impedance response, such as the charge-transfer resistance and double-layer capacitance, with the progress of corrosion in sour corrosive environments is called electrochemical impedance spectroscopy (EIS) evolution. A conventional three-electrode configuration was employed, which included a saturated calomel reference electrode, a graphite counter electrode, and the test specimen as a working electrode, and was linked to a potentiostat. The electrolyte was a 3.5 wt% solution of NaCl, which was saturated with CO_2 (0.1 MPa) and H_2S (0.05 MPa) and kept at 80°C, which approximates the downhole conditions experienced in sour environments [27, 28].

Tafel extrapolation potentiodynamic polarization tests were conducted in a potential-to-open circuit within a range of ± 250 mV relative to the open circuit (scan rate 1 mV/s, N-1). Electrochemical parameters and material constants were used to determine the corrosion rate. EIS was performed in the 10^5 - 10^{-2} Hz AC amplitude (10 mV) in 10^{-1} -1 Hz, and the obtained Nyquist and Bode plots were analyzed with equivalent circuit modelling to determine the charge-transfer resistance and double-layer capacitance [28, 29]. These parameters were used to obtain quantitative information on the passive film stability and corrosion kinetics during the mixed CO_2/H_2S transfer.

2.5 Microstructural characterization

The microstructure of the experiment was characterized using a microscope. Both secondary and backscattered electron modes and high-resolution scanning electron microscopy (SEM) were used as microstructural and fractographic analysis techniques. The morphologies of the fractures were studied to determine the predominant fracture mechanisms, including cleavage, intergranular cracks, and ductile dimples [30].

The grain size, crystallographic texture, and phase distribution in duplex stainless steel were determined using electron backscatter diffraction (EBSD), which enabled a correlation between the microstructure, hydrogen trapping, and crack deflection behavior. Elemental analysis via energy-dispersive X-ray spectroscopy (EDS) demonstrated that the corrosion and pitting precipitation initiation sites as inclusion types included MnS, segregation bands, and bands of both types [27, 28].

2.6 Physics-informed machine learning framework

A hybrid physics-informed machine-learning (PIML) framework was developed by introducing two constitutive relationships into the learning framework: fatigue crack growth kinetics and temperature-dependent corrosion. Experimentally derived parameters are introduced as physical priors or penalty terms in the model objective function to ensure physically consistent predictions [31, 32].

To ensure physically consistent predictions, physical degradation equations were directly incorporated into the loss function of the developed LSTM network using a physics-informed learning approach. The total loss function was formed by blending data-informed loss with physics-informed loss using distinct weighting for both losses.

$$L_{total} = L_{data} + L_f \lambda_{fatigue} + L_c \lambda_{corrosion}$$

where, L_{data} is the mean squared error between the predicted degradation state and values measured in the laboratory. Constraint $L_{fatigue}$ ensures that Paris' law of fatigue crack growth is satisfied. This is evident by:

$$L_{fatigue} = ||(da/dN)_{pred} - C(\Delta K)^m||^2$$

Consistent with Section 2.1.1, da/dN is the growth rate of the fatigue crack, ΔK is the range of the stress intensity factor, and C and m depend on the material.

Arrhenius-type corrosion kinetics dealt with in Section 2.1.2 are employed to obtain the constraint related to corrosion, that is:

$$L_{corrosion} = ||CR(T)_{pred} - A\ exp(-E_a / RT)||^2$$

where, $CR(T)$ is the temperature-dependent corrosion rate, A is the pre-exponential factor, E_a is the activation energy, R is the universal gas constant, and T is the absolute temperature. Learning is influenced by fatigue and corrosion constraints, with the weighting factors λ_f and λ_c determining the degree of influence of one factor on the other.

This is a combination of the stress amplitude, partial pressure of the gases, corrosion current density, charge-transfer resistance, and mechanical properties. Convolutional neural networks were used to process image-based features

formed from SEM and EBSD datasets, and long short-term memory (LSTM) networks were used to model time-dependent degradation signals, that is, EIS evolution and crack propagation histories [33, 34].

The tabular data baseline algorithms were gradient-boosted decision trees and random forest models, and accuracy, R2, and RMSE were used to evaluate the models. Neural networks, probabilistic calibration, Monte Carlo dropout, and isotonic regression were used to estimate uncertainty [31].

2.7 Digital twin implementation

A lightweight platform named the digital twin framework was developed to couple physics-informed machine learning models with the objective of realizing a constantly changing Pipeline Health Index (PHI). The integrity of the entire OCTG system is represented by the PHI, which is a scalar metric with normalized values between 0 and 1. A value of 1 or close to 1 indicates that the system is healthy, whereas a value of 0 or close to 0 indicates that the system has either severely failed or is about to fail. All real-time information related to the downhole pressure, temperature, or fluids was automatically ingested by the platform.

A risk-based maintenance model was optimized to minimize the projected lifecycle costs and avoid premature failures. Digital twins allow the evaluation of mitigation measures, such as changing the operating pressures or the dosage of an inhibitor in scenario analysis, before applying them in practice [31, 34]. This combination of physics-based intelligence and digital analytics provides a framework for real-time decision-making and adaptive maintenance in sour service environments.

3. RESULTS AND DISCUSSION

3.1 Mechanical performance

The average values of the data collected from the three samples under similar loading conditions for all three alloys are presented in Table 1 and Figure 1. The data show improved values of both strength and ductility as a result of advancements in the alloy composition and microstructure.

Table 1. The tensile properties of all materials in this study

Material	Yield Strength (MPa)	UTS (MPa)	Elongation (%)
API X70	482 ± 14	623 ± 17	12.4 ± 1.6
22Cr Duplex SS	552 ± 11	748 ± 19	25.7 ± 2.8
Inconel 625	603 ± 9	903 ± 23	39.6 ± 3.5

API X70 carbon steel has moderate strength and low ductility, which are typical of ferritic-pearlitic microalloyed steels commonly used as standard OCTG casing and line pipe products [13, 18]. The yield strength of 482 MPa and elongation of 12.4 percent are in line with the reported data on the yield strength of hydrogen-exposed microalloyed steels, where plasticity is decreased by embrittlement and segregation of carbide at the grain boundaries [20]. These microstructural constraints are commonly associated with premature fatigue crack propagation during sour service, which is also the case for comparable X-series steels [27].

22Cr duplex stainless steel, on the other hand, has much better strength and ductility. The austenitic-ferritic dual structure improves the resistance to dislocation motion and strain accommodation, which leads to a yield strength of 552 MPa, ultimate strength of 748 MPa, and elongation of 25.7. These findings are consistent with those of Kılınç et al. [30] and Sun et al. [27], who demonstrated that duplex steels can maintain their toughness and mechanical integrity during simultaneous exposure to CO_2/H_2S because of their balanced phase distribution.

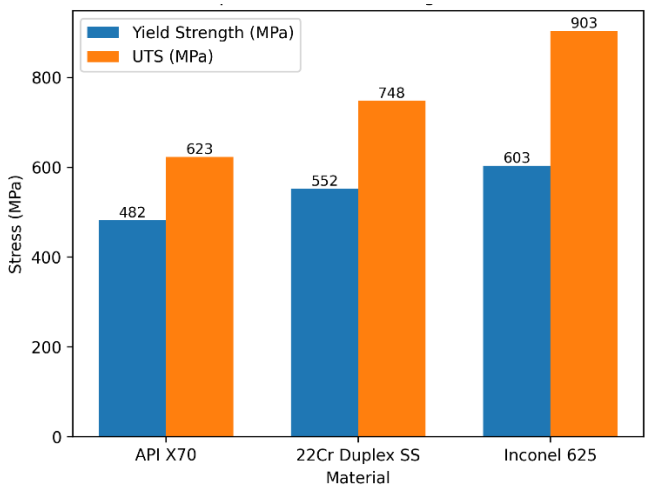

Figure 1. Comparison of yield strength and ultimate tensile strength (UTS) for API X70, 22Cr duplex stainless steel, and Inconel 625

The large elongation is also evidence of the effective trapping of hydrogen and deflection of cracks at the ferrite-austenite boundaries, enhancing their resistance to localized stress corrosion [28].

Inconel 625 exhibited the best performance, with a yield strength of 603 MPa, ultimate tensile strength of 903 MPa, and elongation of 39.6 percent. The cause of this behavior is the solid-solution strengthening of Mo and Nb, coupled with dislocated γ′ and γ″ precipitates, which increase the creep and fatigue strength [29, 31]. Solovyeva et al. [29] reported that thermal stability and plasticity of Inconel 625 render it highly appropriate in high-temperature and high-H 2 S conditions in which typical steels tend to lose their ductility quickly. Moreover, its high microstructural refinement-fatigue endurance correlation promotes previous computational forecasts of digital twins and physics-informed models [7, 21, 22, 31, 33].

The strengthening and ductility improvement between API X70 and 22Cr Duplex and Inconel 625 prove that the enhancement is possible because of the design of alloys and phase control.

This confirms that high-nickel and duplex systems are more applicable to sour-service OCTG components that require high load capability and long-term dimensional stability [11, 21, 22].

3.2 Electrochemical behavior

The electrochemical data presented in Table 2 and Figure 2 were derived from Tafel polarization and EIS experiments performed in a 3.5% NaCl solution saturated with CO_2 (0.1 MPa) and H_2S (0.05MPa) at 80°C. As shown in Figures 3 and 4, there was a strong composition dependence of the corrosion rate and passive layer lifetime.

Table 2. Electrochemical parameters in CO_2/H_2S-saturated brine at 80°C

Material	Icorr (μA/cm²)	Rct (kΩ·cm²)	Corrosion Rate (mm/year)
API X70	30.1	0.93	0.349
22Cr Duplex SS	7	4.06	0.066
Inconel 625	1.1	11.85	0.011

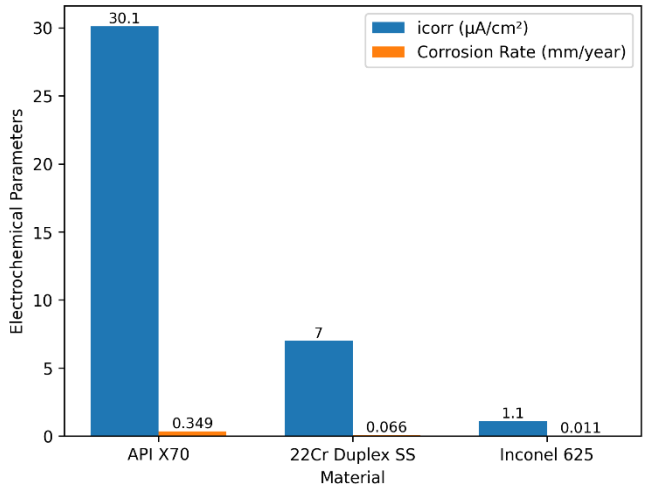

Figure 2. Comparison of corrosion current density (icorr) and corrosion rate for the investigated materials in CO_2/H_2S-saturated brine at 80°C

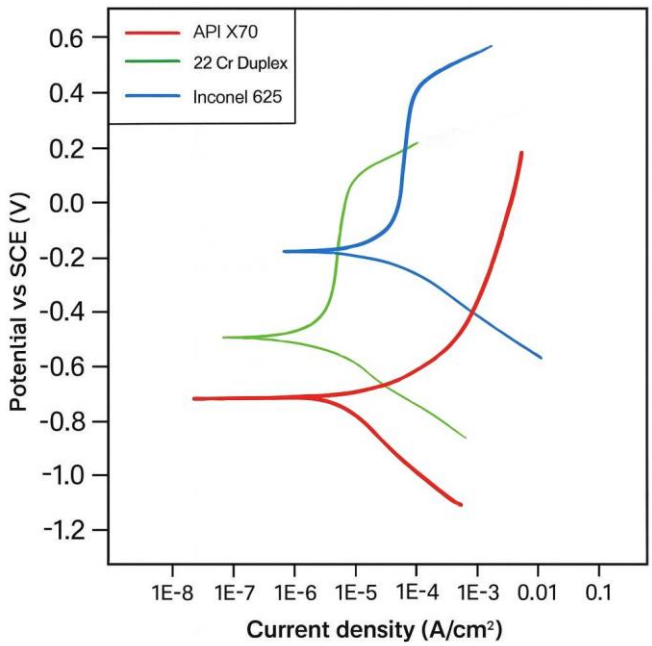

Figure 3. Tafel polarisation curves of API X70, 22Cr duplex steel and Inconel 625

API X70 carbon steel recorded the highest corrosion current density (30.1 μA/cm²) and lowest charge-transfer resistance (0.93 kΩ cm²), resulting in a corrosion rate of approximately 0.349 mm/year. This effect is normal in low-alloy ferritic steels in sour environments, where the presence of CO_2 and H_2S destabilizes the $FeCO_3$/FeS protective layers, resulting in localized film breakdown and accelerated anodic dissolution [27, 29]. The interaction between CO_2 and H_2S enhances the cathodic hydrogen evolution reaction, increasing surface acidity and causing pit nucleation [27, 29].

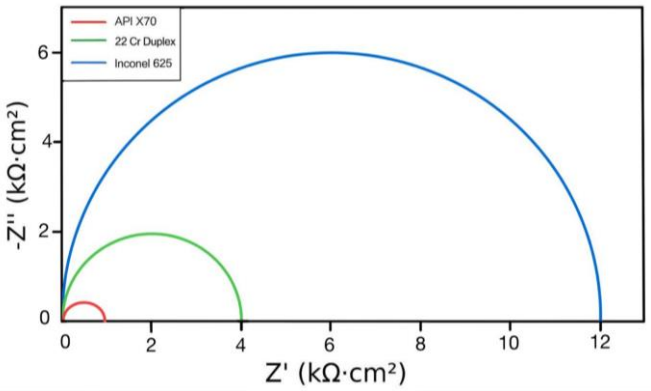

Figure 4. Nyquist impedance plots of API X70, 22Cr duplex steel and Inconel 625

Nyquist plots typically have a small semicircle diameter of X70, indicating that the main control of corrosion is charge transfer rather than diffusion, as observed by Solovyeva et al. [29].

The 22Cr duplex stainless steel exhibited a significantly low corrosion current density (7.0 μA/cm²) and high Rct (4.06 kΩ cm²), which was equivalent to a corrosion rate of 0.066 mm/year.

This is because it forms a small Cr_2O_3–$FeCr_2O_3$ passive layer, which is resistant to the CO_2-H_2S combination [27, 30]. Kılınç et al. [30] stated that duplex stainless steels form a duplex oxide/sulfide coating that keeps the structure intact despite the long exposure period and drastically minimizes hydrogen ingress. In addition, the ferrite–austenite interface provides a network of hydrogen traps, reduces embrittlement, and controls the anodic dissolution rate [28, 33].

Inconel 625 exhibited the best corrosion resistance, lowest corrosion current density (1.1 μA/cm²), and maximum Rct (11.85 kΩ cm²); consequently, an exceedingly low corrosion rate of 0.011 mm/year was obtained. This is linked to the development of a thick NiO-Cr_2O_3-MoO_3 passive layer, which offers better resistance to both chloride and sulfide cation permeabilities [29, 31]. According to Wu et al. [33] and Meza et al. [34], Ni-based superalloys exhibit diffusion-controlled reactions to impedance under the conditions of H_2S/CO_2, which implies that corrosion is constrained by slow ionic conduction through the protective film rather than by charge-transfer reactions.

The steep phase angle in the Bode diagrams and the large diameter of the semicircle in the Nyquist plots attest to the fact that the signature of stable passive behavior is in line with the predictions of the long-term behavior of the digital twin in sour service environments [31, 34].

In general, Inconel 625 exhibits a higher resistance to corrosion than 22Cr Duplex SS and API X70, which is negatively proportional to icorr and directly proportional to Rct. These findings clearly show that more protective oxide-sulfide layers are formed in the presence of higher Cr, Ni, and Mo alloys, which significantly decreases the rate of corrosion in CO_2/H_2S settings [27-30].

Moreover, the parameters obtained in the polarization and EIS analyses (icorr, Rct, and corrosion rate) are crucial input parameters in the next physics-informed machine learning and

digital twin models applied in predictive degradation modelling and reliability measurements [21, 31, 33, 34].

3.3 Microstructural analysis

High-resolution SEM enabled microstructural analysis to provide the necessary information on the fracture mechanisms that dominate the behavior of the three alloys examined under sour service conditions. As shown in Figure 5, SEM observations were used to complete the mechanical and electrochemical observations, showing how the different fracture morphologies, including brittle cleavage in API X70, mixed-mode characteristics in 22Cr duplex steel, and fully ductile microvoid coalescence in Inconel 625, were determined by the underlying deformation modes and environmental susceptibility of each material.

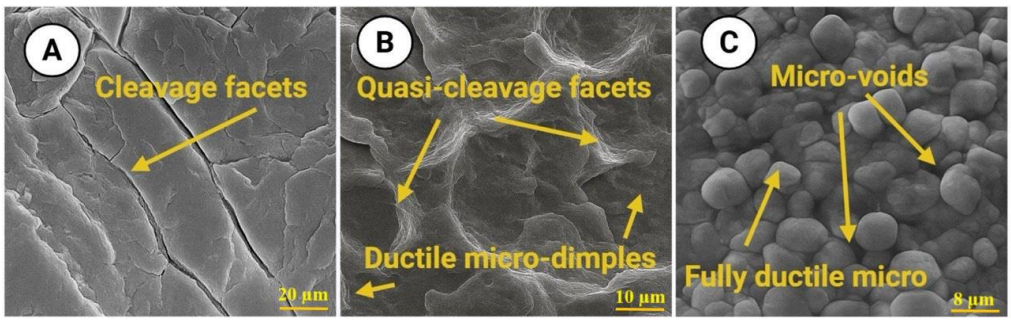

Figure 5. Fractographic features: (a) brittle cleavage in API X70, (b) mixed quasi-cleavage and ductile dimples in 22Cr duplex steel, and (c) fully ductile microvoid coalescence in Inconel 625

For API X70 carbon steel, the SEM fractograph showed a strong cleavage facet with secondary cleavages, representing a predominantly brittle and transgranular fracture process. The angular fracture planes and scanty plastic relief indicate that hydrogen-assisted cracking and localized anodic dissolution work together to propagate cracks under stress in a brittle manner. These fracture features can be attributed to the fact that CO_2/H_2S co-exposure disrupts the protective $FeCO_3/FeS$ coating and increases crack propagation in ferritic steels [27, 28].

The 22Cr duplex stainless steel exhibited a mixed-mode fracture morphology with quasi-cleavage facets and ductile microdimples. This mixture results from the bipolarity of duplex alloys, with the ferritic component being more prone to fracture and the austenitic component being more prone to plastic deformation. This phase-selective fracture behavior increases crack bending, energy capture, and toughness, as observed in duplex alloys exposed to hostile environments [30, 31].

In contrast, Inconel 625 exhibited a fully ductile fracture morphology typified by evenly dispersed hemispherical dimples and definite signs of microvoid coalescence. The lack of brittle characteristics or secondary cracking emphasizes the remarkable hydrogen uptake and localized corrosion resistance of the alloy. This ductile nature is consistent with the long-established effect of γ′/γ″ strengthening precipitates in Ni-based superalloys, which facilitates homogeneous deformation and slower crack growth, even under harsh sour conditions [33, 34].

As shown by the SEM evidence, brittle cleavage (API X70), mixed-mode behavior (22Cr duplex stainless steel), and full ductile microvoid coalescence (Inconel 625) were distinctly connected and directly corresponded to the trends in the mechanical, electrochemical, and degradation properties of the three materials.

3.4 Physics-informed AI model performance

Table 3 shows that the evaluated machine-learning architectures exhibited a performance gradient that was specific to their inherent differences in their ability to describe the degradation processes in sour-service applications of OCTG. Random Forest achieved an average degree of prediction fidelity (accuracy 0.85 ± 0.03; $R^2 = 0.82 \pm 0.04$), as expected, because tree-based ensembles have been shown to be highly predictive with tabular, non-sequential features, but ineffective with highly path-dependent material degradation processes [8]. This constraint is particularly pertinent to hydrogen-aided fatigue and corrosion-based damage, where sudden degradation does not occur.

Table 3. Comparative performance of machine learning models for failure mode classification and remaining useful life prediction

Model Architecture	Primary Task	Classification Accuracy	R^2 (Life Prediction)
Random Forest	Failure mode classification	0.85 ± 0.03	0.82 ± 0.04
XGBoost	Failure mode classification	0.88 ± 0.02	0.87 ± 0.03
Physics-Informed long short-term memory (LSTM)	Integrated prediction	0.93 ± 0.02	0.92 ± 0.03

XGBoost performance was better (accuracy 0.88 ± 0.02; $R^2 = 0.87 \pm 0.03$), and this result is consistent with the results of other researchers who found that gradient-boosted decision trees outperform traditional ensembles under the condition of nonlinear and multi-interaction relationship of features [9]. Nonetheless, similar to Random Forest, XGBoost still assumes that input samples are independent observations; therefore, it cannot capture temporal aspects, such as crack-growth curves or EIS evolution paths, that control the remaining useful life.

The Physics-Informed LSTM had the greatest predictive power (accuracy 0.93 ± 0.02; $R^2 = 0.92 \pm 0.03$), which reflects the overall advantage of recurrent neural network sequence modelling together with intrinsic physics-based constraints.

This finding confirms the emerging belief that physics-informed architectures are highly effective for improving extrapolation robustness and reducing unphysical material degradation predictions [32, 33]. The LSTM block is trained on long-range temporal dependencies between crack growth histories and the electrochemical evolution of electrochemical evolution data and enforces physics-based penalty terms, which enforce obedience to the mechanistic laws of fracture fatigue kinetics, Arrhenius corrosion acceleration, etc., into a dual constraint learning environment.

Furthermore, the better-than-physical-model performance is also compatible with recent trends in the digital twin literature that discuss the need to adopt a physically grounded AI that ensures reliable functionality in safety-critical systems [31, 34]. Operational decision-making is also critical because its capability of making stable and interpretable predictions is critical in areas where maintenance scheduling and risk mitigation rely on precise remaining useful life (RUL) estimations.

Overall, the performance ranking, Random Forest < XGBoost < Physics-Informed LSTM, is not only experimentally justified in this study but also theoretically consistent with the modern information on degradation modelling, which proves that physics-guided sequential networks provide the most successful basis for OCTG digital-twin integration.

3.5 Digital twin validation and deployment

The verifiability of the physics-informed digital twin was demonstrated by comparing the AI-driven degradation prediction with experimental fatigue, corrosion, and creep data under sour conditions and high temperatures. The additional forecasts of the remaining useful life were not more than approximately 10 percent of the measured values, and the uncertainty bands were able to absorb most of the experimental variations, which presents good model robustness and generalization. The combination of mechanical, electrochemical, and microstructural inputs to make physically consistent predictions and the inclusion of the Paris law and Arrhenius kinetics to avoid non-physical behavior in sparsely populated operating regimes have been achieved [21, 22].

The digital twin translates the predicted rate of degradation into an index of Pipeline Health that is constantly updated, using which real-time maintenance decisions are made. To comply with the dynamic synchronization concepts (as reported by Meza et al. [34]), when the index drops below a certain threshold, automated inspection alerts are produced. Sensitivity analysis, which assessed the modification of the cyclic stress amplitude and partial pressure of H_2S, produced the highest enhancements in the RUL, which is consistent with the findings of sour-service degradation studies [6, 11]. In general, the validated framework is a reliable reproducer of degradation trends and a useful decision-support tool for condition-based maintenance of OCTG systems that can bridge the gap between laboratory characterization and field-scale monitoring of complex service conditions.

4. CONCLUSIONS AND FUTURE PERSPECTIVES

This study proposes an integrated digital twin framework for predicting the rate of degradation and remaining life of OCTG materials under sour and high-temperature conditions, which is grounded in physics principles. One of the novel aspects of this proposed approach is the blending of physically based models of degradation, such as Paris' fatigue law of crack growth and Arrhenius-type models of corrosion kinetics with the sequence-based machine learning framework. This blending allows the results to remain physically sound, intelligible, and robust while maintaining a high degree of accuracy.

It was observed that experiments revealed that Inconel 625 is more robust and corrosion-resistant than 22Cr duplex stainless steel and API X70 carbon steel. This clearly indicates that it is effective under harsh source-service conditions. When combined with the physics-informed LSTM and digital twin framework, the properties established through experiments were useful for precise degradation analysis with differences of no more than 10%.

Despite these encouraging results, the current study has certain limitations. The experimental data used in this study were drawn from a controlled laboratory setting with limited environmental factors, which may not completely capture the complexities of real-world variability. Additionally, the current framework considers that all conditions of exposure are equivalent, without considering the influence of multiphase flow or regionalized damage accumulation.

Future work will be aimed at integrating the proposed framework with sensor data, incorporating spatially resolved damage models, as well as learning/adaptive features. It is expected that further research on multiphysics coupling and uncertainty quantification in the digital twin framework will lead to enhanced prediction capability and application domains for other engineering systems that fall under the safety-critical category.

ACKNOWLEDGEMENT

The authors gratefully acknowledge the support of the University of Anbar and Mustansiriyah University.

REFERENCES

[1] Fedukhin, O.V., Mukha, A.A. (2025). A conceptual framework for a comprehensive industrial equipment reliability management system using predictive analytics. Mathematical Machines and Systems, 2: 67-75. https://doi.org/10.34121/1028-9763-2025-2-67-75

[2] Avevor, J., Adeniyi, M., Eneejo, L., Selasi, A. (2024). Machine learning-driven predictive modeling for FRP strengthening structural elements. A review of AI-based damage detection. Fatigue Prediction, and Structural Health Monitoring. International Journal of Scientific Research and Modern Technology, 3(8): 1-20. https://doi.org/10.38124/ijsrmt.v3i8.420

[3] Laroche, B.J., II, York, T.L. (2024). An analysis of database applications for digital twin data fusion and knowledge management. Master's thesis. Naval Postgraduate School.

[4] White, M., Ellington, S. (2022). Adoption of digital twin within the department of the navy. Doctoral dissertation. Acquisition Research Program. https://dair.nps.edu/handle/123456789/4777.

[5] Agostinelli, S. (2023). Optimization and management of microgrids in the built environment based on intelligent digital twins. Doctoral dissertation. Sapienza University of Rome. https://iris.uniroma1.it/retrieve/76712fbd-6876-4050-8c46-e149c2ed733f/Tesi_dottorato_Agostinelli.pdf.

[6] Koirala, B., Cai, H., Khayatian, F., Munoz, E., An, J.G., Mutschler, R., Sulzer, M., De Wolf, C., Orehounig, K. (2024). Digitalization of urban multi-energy systems – Advances in digital twin applications across life-cycle phases. Advances in Applied Energy, 16: 100196. https://doi.org/10.1016/j.adapen.2024.100196

[7] Agnusdei, G.P., Elia, V., Gnoni, M.G. (2021). Is digital twin technology supporting safety management? A bibliometric and systematic review. Applied Sciences, 11(6): 2767. https://doi.org/10.3390/app11062767

[8] Cubillo, A., Perinpanayagam, S., Esperon-Miguez, M. (2016). A review of physics-based models in prognostics: Application to gears and bearings of rotating machinery. Advances in Mechanical Engineering, 8(8). https://doi.org/10.1177/1687814016664660

[9] Kim, B., Azevedo, V., Thuerey, N., Kim, T., Gross, M., Solenthaler, B. (2018). Deep fluids: A generative network for parameterized fluid simulations. Computer Graphics Forum, 38(2): 59-70. https://doi.org/10.48550/arXiv.1806.02071

[10] Tibaduiza Burgos, D.A., Gomez Vargas, R.C., Pedraza, C., Agis, D., Pozo, F. (2020). Damage identification in structural health monitoring: A brief review from its implementation to the use of data-driven applications. Sensors, 20(3): 733. https://doi.org/10.3390/s20030733

[11] Liu, X., Furrer, D., Kosters, J., Holmes, J. (2018). Vision 2040: A roadmap for integrated, multiscale modeling and simulation of materials and systems.

[12] Ewart, P. (2019). A comparison of processing techniques for producing prototype injection moulding inserts. https://researcharchive.wintec.ac.nz/id/eprint/7270/.

[13] Mohammed, A.I., Bartlett, M., Oyeneyin, B., Kayvantash, K., Njuguna, J. (2022). Multi-criteria material selection for casing pipe in shale gas wells application. Journal of Petroleum Exploration and Production Technology, 12(12): 3183-3199. https://doi.org/10.1007/s13202-022-01506-0

[14] Bernal, M.P., Bescós, B., Burgos, L., Bustamante, M.Á., et al. (2015). Evaluation of manure management systems in Europe. https://upcommons.upc.edu/handle/2117/88745.

[15] Zewdie, T.A., Fanta, S., Alemayehu, M., Alemayehu, G., Adgo, E., Nyssen, J., Delele, M., Verboven, P., Nicolai, B. (2019). Effect of curing conditions and harvesting stage of maturity on Ethiopian onion bulb drying properties. In 7th European Drying Conference, pp. 429-435. http://hdl.handle.net/1854/LU-8660344.

[16] Ceschin, F., Vezzoli, C., Zhang, J. (2010). Sustainability in design: Now! Challenges and opportunities for design research, education and practice in the XXI century. In Proceedings of the LeNS Conference, Bangalore, India. http://bura.brunel.ac.uk/handle/2438/6726.

[17] Animashaun, T.A., Sunday, O., Ogunleye, E., Agbahiwe, O.K., et al. (2025). AI-powered digital twin platforms for next-generation structural health monitoring: From concept to intelligent decision-making. Journal of Engineering Research and Reports, 27(10): 12-37. https://doi.org/10.9734/jerr/2025/v27i101652

[18] Negi, A., Elkhodbia, M., Barsoum, I. (2025). A coupled phase-field modeling framework for predicting sulfide stress cracking and pipe burst in sour environment. Theoretical and Applied Fracture Mechanics, 140: 105099. https://doi.org/10.1016/j.tafmec.2025.105099

[19] Jiang, S., Wang, J., Zhao, B., Zhang, E. (2024). The study on fatigue crack growth rate of 4130X material under different hydrogen corrosion conditions. Materials, 17(1): 257. https://doi.org/10.3390/ma17010257

[20] Zhao, T., Liu, Z., Xu, X., Li, Y., Du, C., Liu, X. (2019). Interaction between hydrogen and cyclic stress and its role in fatigue damage mechanism. Corrosion Science, 157: 146-156. https://doi.org/10.1016/j.corsci.2019.05.028

[21] Farhat, H., Altarawneh, A. (2025). Physics-informed machine learning for intelligent gas turbine digital twins: A review. Energies, 18(20): 5523. https://doi.org/10.3390/en18205523

[22] Parsa, S.M. (2025). Physics-informed machine learning meets renewable energy systems: A review of advances, challenges, guidelines, and future outlooks. Applied Energy, 402(Part A): 126925. https://doi.org/10.1016/j.apenergy.2025.126925

[23] ASTM International. (2022). Standard test methods for tension testing of metallic materials (ASTM E8/E8M-22). ASTM International. https://doi.org/10.1520/E0008_E0008M-22

[24] ASTM International. (2015). Standard practice for conducting force-controlled constant-amplitude axial fatigue tests of metallic materials (ASTM E466-15). ASTM International. https://doi.org/10.1520/E0466-15

[25] ASTM G1-03(2017)e1. (2017). Standard practice for preparing, cleaning, and evaluating corrosion test specimens. https://doi.org/10.1520/G0001-03R17E01

[26] ASTM E139-11. (2018). Standard test methods for conducting creep, creep-rupture, and stress-rupture tests of metallic materials. https://doi.org/10.1520/E0139-11R18

[27] Sun, C., Ding, T., Sun, J., Lin, X., Zhao, W., Chen, H. (2023). Insights into the effect of H_2S on the corrosion behavior of N80 steel in supercritical CO_2 environment. Journal of Materials Research and Technology, 26: 5462-5477. https://doi.org/10.1016/j.jmrt.2023.08.277

[28] Yue, Y., Yin, Z., Li, S., Zhang, Z., Zhang, Q. (2025). Corrosion behavior of mild steel in various environments including CO_2, H_2S, and their combinations. Metals, 15(4): 440. https://doi.org/10.3390/met15040440

[29] Solovyeva, V.A., Almuhammadi, K.H., Badeghaish, W.O. (2023). Current downhole corrosion control solutions and trends in the oil and gas industry: A review. Materials, 16(5): 1795. https://doi.org/10.3390/ma16051795

[30] Kılınç, B., Kocaman, E., Şen, Ş., Şen, U. (2021). Effect of vanadium content on the microstructure and wear behavior of $Fe(13-x)V_xB_7$ ($x = 0–5$) based hard surface alloy layers. Materials Characterization, 179: 111324. https://doi.org/10.1016/j.matchar.2021.111324

[31] Munko, M.J., Vidmar, M., Brádaigh, C.M.Ó., Cuthill, F., Camacho, M.A.V., Dubon, S.L. (2024). Do digital twins require physical simulations? A study of developing digital twins with varying reliance on physics-based models. In 2024 IEEE International Conference on Engineering, Technology, and Innovation (ICE/ITMC), Funchal, Portugal, pp. 1-8.

https://doi.org/10.1109/ICE/ITMC61926.2024.10794252
[32] Dourado, A., Viana, F.A.C. (2019). Physics-informed neural networks for corrosion-fatigue prognosis. Annual Conference of the PHM Society, 11(1). https://doi.org/10.36001/phmconf.2019.v11i1.814
[33] Wu, T., Miao, X., Song, F. (2025). Residual strength prediction of corroded pipelines based on physics-informed machine learning and domain generalization. npj Materials Degradation, 9: 12. https://doi.org/10.1038/s41529-025-00561-2
[34] Meza, E.B.M., Souza, D.G.B.D., Copetti, A., Sobral, A.P.B., Silva, G.V., Tammela, I., Cardoso, R. (2024). Tools, technologies and frameworks for digital twins in the oil and gas industry: An in-depth analysis. Sensors, 24(19): 6457.https://doi.org/10.3390/s24196457

NOMENCLATURE

OCTG	Oil country tubular goods
PIML	Physics-informed machine learning
PI-LSTM	Physics-informed long short-term memory model
DT / Digital Twin	Real-time virtual replica of physical system
API X70	Carbon steel used for pipelines
22Cr Duplex SS	22% chromium duplex stainless steel
Inconel 625	Nickel-based superalloy
H_2S	Hydrogen sulfide
CO_2	Carbon dioxide
SCC	Stress corrosion cracking
SSC	Sulfide stress cracking
HIC	Hydrogen-induced cracking
EIS	Electrochemical impedance spectroscopy
SEM	Scanning electron microscopy
EBSD	Electron backscatter diffraction
EDS	Energy-dispersive X-ray spectroscopy
icorr	Corrosion current density
Rct	Charge-transfer resistance
ΔK	Stress intensity factor range
da/dN	Fatigue crack growth rate
RUL	Remaining useful life